Decoherence and interactions in an electronic Mach-Zehnder interferometer

J. T. Chalker,[1] Yuval Gefen,[1,2] and M. Y. Veillette[1]

[1]*Theoretical Physics, Oxford University, 1, Keble Road, Oxford OX1 3NP, United Kingdom*
[2]*Department of Condensed Matter Physics, Weizmann Institute of Science, Rehovot 76100, Israel*
(Received 8 March 2007; revised manuscript received 11 July 2007; published 13 August 2007)

We develop a theoretical description of a Mach-Zehnder interferometer built from integer quantum Hall edge states, with an emphasis on how electron-electron interactions produce decoherence. We calculate the visibility of interference fringes and noise power as a function of bias voltage and of temperature. Interactions are treated exactly by using bosonization and considering edge states that are only weakly coupled via tunneling at the interferometer beam splitters. In this weak-tunneling limit, we show that the bias dependence of Aharonov-Bohm oscillations in source-drain conductance and noise power provides a direct measure of the one-electron correlation function for an isolated quantum Hall edge state. We find the asymptotic form of this correlation function for systems with either short-range interactions or unscreened Coulomb interactions, extracting a dephasing length ℓ_φ that varies with temperature T as $\ell_\varphi \propto T^{-3}$ in the first case and as $\ell_\varphi \propto T^{-1}\ln^2(T)$ in the second case.

I. INTRODUCTION

Several striking phenomena in electronic Mach-Zehnder interferometers built from integer quantum Hall edge states have been reported in a sequence of recent experimental papers.[1–4] The central observation[1] is of interference fringes in the differential source-drain conductance of the interferometer, as the magnetic flux enclosed between its arms is changed. The high contrast of these fringes (up to 60%) is remarkable in view of the relatively large size (around 10 μm) of the interferometer. The interference fringes are suppressed as the sample temperature is increased or as the system is driven out of equilibrium by a finite source-drain bias. In each case, this suppression offers a window onto dephasing processes in the system, and such processes are the subject of this paper.

These experiments form part of a larger effort to understand and make use of interference effects in quantum Hall systems. In the context of the fractional quantum Hall effect, challenges include detection of anyonic phases for quasiparticles[5–11] and, more ambitiously, of non-Abelian quasiparticle phases.[11] Against this background, it is clearly important to have a proper understanding of the simpler interaction effects expected in integer quantum Hall systems, and our aim in the following is to establish a theoretical description of some of these effects.

The design of an electronic Mach-Zehnder interferometer is illustrated in Fig. 1: two edge states, which propagate in the *same* sense, meet at two places where they are coupled by quantum point contacts, which act as the equivalent of the beam splitters used in the optical version of the interferometer. An attractive feature of the Mach-Zehnder arrangement is that each electron passes only once through the interferometer, and this simplifies the theoretical analysis. In contrast, for a Fabry-Perot design,[12] particles may execute multiple circuits of the interferometer before exiting.

A body of earlier theoretical work[13–18] on electronic Mach-Zehnder interferometers built from integer quantum Hall edge states has treated sources of dephasing that are distinct from the edge states themselves. These sources of dephasing are represented by a fictitious voltage probe[16] or by a fluctuating electrostatic potential,[13–15,17,18] which may have various origins, including the movement of charged impurities within the sample and thermal or nonequilibrium electromagnetic radiation in the sample's surroundings. Our concern in this paper is instead with dephasing that is *intrinsic* to the interferometer and that arises from interactions between electrons in the edge states themselves. Some previous discussions[1,14] have emphasized the distinction between *fast* and *slow* potential fluctuations, as compared to the flight time for electrons passing through the interferometer. Within that classification, we deal here with fast fluctuations. We are motivated by several considerations. First, as we show, intrinsic dephasing is a useful experimental probe of electron-electron interactions in integer quantum Hall edge states. Second, since external sources of dephasing can, at least in principle, be reduced in experiment, intrinsic contributions should ultimately dominate. And third, in relation to recent experiments, while temperature-dependent dephasing may plausibly arise from either external or intrinsic sources, we believe that bias-dependent dephasing most likely results from an intrinsic mechanism.

Our approach is to start from a system without tunneling at the interferometer quantum point contacts. In this limit,
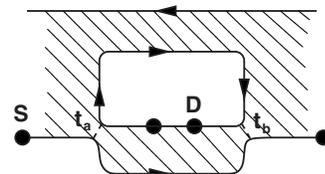

FIG. 1. Sketch of the electronic Mach-Zehnder interferometer. Two quantum Hall edge states are coupled by tunneling at two quantum point contacts. One of these edge states lies at the edge of a Hall bar and starts from source S; the other encircles an antidot within the Hall bar and ends at drain D. Tunneling amplitudes at the point contacts are denoted by t_a and t_b.
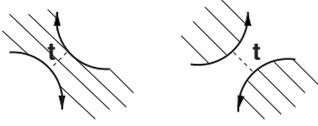
FIG. 2. Action of the tunneling Hamiltonian for a contact that is almost open (left) and for one that is almost pinched off (right); the shaded region is occupied by electrons.
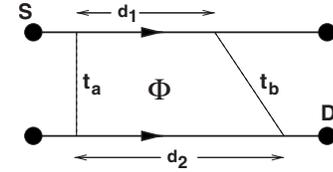

FIG. 3. Schematic view of interferometer, showing arm lengths d_1 and d_2, tunneling amplitudes t_a and t_b, and arrangement of source S and drain D. The magnetic flux enclosed by the two possible electron paths is indicated by Φ.

assuming a confining potential for electrons at the sample edge that rises linearly with position, electron-electron interactions can be handled exactly, using bosonization to obtain a harmonic Hamiltonian for collective edge excitations. For simplicity, we study translation-invariant edges and omit interactions between electrons on different edges. Introducing tunneling into the description, since the tunneling Hamiltonian is not quadratic in boson operators, we treat it perturbatively, calculating source-drain conductance and noise power for the interferometer at leading order in tunneling amplitudes. Such an approach is good when both point contacts are almost open and the reflection probability is small, as illustrated in Fig. 1, and when they are close to pinch-off and the transmission probability is small; for the two cases, the tunneling Hamiltonian acts as sketched in Fig. 2. In this way, we bracket from both sides the regime in which transmission and reflection probabilities are similar.

It is a familiar fact that interactions have rather limited consequences in integer quantum Hall edge states, in the sense that the asymptotic low-energy behavior is that of a Fermi liquid rather than a Luttinger liquid.[19] Indeed, if interactions are modeled by a short-range potential, their only effect is to renormalize the edge-state velocity. More generally, interactions generate a nonlinear dispersion relation for collective modes. The dispersion, in turn, means that a wave packet representing an electron that has tunneled into an edge will spread as it propagates. It is this spreading that gives rise to the dephasing we study here. In the context of an interferometer, we are concerned with what happens during propagation along an interferometer arm. If the arm length is large the propagation time is long and spreading is determined by the low-frequency form of the dispersion relation, which depends on the behavior of the Fourier transform of the interaction potential at small wave vector. As an intermediate step in the calculation of observable quantities, we find the asymptotic, long-distance form of the one-electron correlation function, presenting results for both generic, finite-range interactions and for unscreened Coulomb interactions. From this we obtain the bias dependence of conductance and noise power for the interferometer. Our approach is parallel to recent calculations of the effect of Coulomb interactions on transport between edge states in multilayer quantum Hall systems.[20] We do not consider interedge interactions in special geometries, which may give rise to resonance phenomena as discussed recently in Ref. 21.

Without interactions, Aharonov-Bohm oscillations in conductance contain only the zeroth and first harmonics in Φ/Φ_0, while those of the noise power contain zeroth, first, and second harmonics. From the structure of our calculations, it is apparent that interactions generate higher harmonics for both quantities, albeit at higher orders in our expansion in tunneling amplitudes.

The remainder of the paper is organized as follows. In Sec. II we define our model and the one-electron correlation function for an isolated edge, from which interferometer properties at weak tunneling can be calculated. We derive expressions for conductance and noise power in Sec. III. We discuss asymptotics of the correlation function in Sec. IV and use these in Sec. V to determine visibility of interference fringes in conductance as a function of bias voltage and temperature. We discuss our findings in Sec. VI.

II. MODEL

We consider an idealized version of the experimental system shown in Fig. 3, with the model Hamiltonian $\mathcal{H}=\mathcal{H}_0 + \mathcal{H}_{\text{tun}} + \mathcal{H}_{\text{int}}$. Here, the single-particle terms $\mathcal{H}_0$ and $\mathcal{H}_{\text{tun}}$ represent free motion along each edge and interedge electron tunneling, respectively, while $\mathcal{H}_{\text{int}}$ describes electron interactions within an edge. We write the Hamiltonian in terms of the electron creation operator $c_{qm}^{\dagger}$ for a state with wave vector q on the edge $m=\{1,2\}$, defining one-particle basis states for an edge of length L so that $q=2\pi n_q/L$, where n_q is integer. The creation operator at a point x on the edge m is

$$\psi_m^{\dagger}(x) = \frac{1}{\sqrt{L}} \sum_{q=-\infty}^{\infty} e^{-iqx} c_{qm}^{\dagger}. \qquad (1)$$

We normal order the Hamiltonian with respect to a vacuum in which states are occupied for $q \leq 0$ and empty otherwise. Taking a strictly linear electron dispersion relation, the Hamiltonian for free motion is

$$\mathcal{H}_0 = -i\hbar v \sum_{m=1,2} \int dx \, :\psi_m^{\dagger}(x)\partial_x\psi_m(x): , \qquad (2)$$

where v is the edge velocity; the consequences of curvature in this dispersion relation are discussed in Sec. IV. We consider narrow quantum point contacts, so that the tunneling occurs at a single position, with

$$\mathcal{H}_{\text{tun}} = t_a\psi_1^{\dagger}(0)\psi_2(0) + t_b\psi_1^{\dagger}(d_1)\psi_2(d_2) + \text{H.c.} \qquad (3)$$

The electron-electron interaction energy within each edge can be written in terms of the density operator $\rho_m(x) = \psi_m^{\dagger}(x)\psi_m(x)$. Assuming a translation-invariant two-particle potential $U(x-x')$ we have

$$\mathcal{H}_{\text{int}} = \frac{1}{2} \sum_{m=1,2} \int \int dx dx' : \rho_m(x) U(x-x') \rho_m(x'):. \quad (4)$$

The phase arising from the enclosed flux Φ appears in the tunneling amplitudes: $t_a t_b^* = |t_a t_b^*| e^{i\theta}$ where $\theta = \Phi/\Phi_0$ and $\Phi_0 = h/e$ is the flux quantum.

A. Bosonized Hamiltonian

We bosonize the Hamiltonian in the standard way, expressing $\mathcal{H}_0 + \mathcal{H}_{\text{int}}$ in terms of harmonic collective modes. Boson creation operators are defined (see, for example, Ref. 22) as

$$b_{qm}^\dagger = \frac{i}{\sqrt{n_q}} \sum_k c_{k+q,m}^\dagger c_{k,m} \quad (5)$$

for $q > 0$. These boson operators satisfy the canonical commutation relation

$$[b_{qm}, b_{kn}^\dagger] = \delta_{qk} \delta_{mn}. \quad (6)$$

Fourier transforming the interaction potential and expressing the result as a velocity, we introduce

$$u(q) = \frac{1}{2\pi\hbar} \int dx e^{iqx} U(x). \quad (7)$$

The Hamiltonian in the absence of tunneling is $\mathcal{H}_1 \equiv \mathcal{H}_0 + \mathcal{H}_{\text{int}}$, with

$$\mathcal{H}_1 = \sum_{m=1,2} \left[\frac{\pi\hbar v}{L} \hat{N}_m(\hat{N}_m + 1) + \sum_{q>0} \hbar\omega(q) b_{qm}^\dagger b_{qm} \right], \quad (8)$$

where the collective mode frequency is $\omega(q) = q[v + u(q) - u(0)]$ and the number operator for edge m is $\hat{N}_m = \int dx \rho_m(x)$. Linearizing the dependence on $\hat{N}_m$ about the mean value $\langle \hat{N}_m \rangle$, expressed in terms of the chemical potential via $\mu_m = 2\pi\hbar v \langle \hat{N}_m \rangle / L$, and omitting a constant, we have

$$\mathcal{H}_1 = \sum_{m=1,2} \left[\mu_m \hat{N}_m + \sum_{q>0} \hbar\omega(q) b_{qm}^\dagger b_{qm} \right]. \quad (9)$$

We will focus on the limit in which the interferometer arm lengths d_1 and d_2 are much larger than the range of interactions and will therefore be concerned with the dispersion relation at small $\omega(q)$, and hence small q. We consider two alternative forms for interactions: generic short-range interactions and unscreened Coulomb interactions. The first is appropriate for an edge state defined by a metallic gate, since in this case charges in the gate will screen interactions between electrons in the edge state. The second case is appropriate for an edge state defined by etching.

For short-range interactions we write $u(0) - u(q) = v(bq)^{n-1} + \mathcal{O}(q^n)$, where the length b characterizes a combination of the range and strength of interactions. Since the Fourier transform of a short-range interaction potential is analytic at $q=0$, one expects $n=3$. In this way, an interaction $U(x)$ of strength U_0 and range b_0 is described completely for our purposes by the length $b \sim b_0(U_0 b_0/\hbar v)^{1/2}$.

For the Coulomb interaction, regularized at short distances by a finite width a of edge states, with the form

$$U(x) = \frac{e^2}{4\pi\epsilon_0\epsilon_r} \frac{1}{\sqrt{x^2 + a^2}}, \quad (10)$$

one has

$$u(q) = u K_0(aq), \quad (11)$$

where K_0 is the hyperbolic Bessel function and $u = e^2/(2\pi)^2 \hbar \epsilon_0 \epsilon_r$. At small q one has in this case $\omega(q) = vq + uq \ln([aq]^{-1})$.

We emphasize that in our treatment of long-wavelength edge excitations, all interaction effects appear in the dispersion relation $\omega(q)$ for collective modes via the potential $u(q)$. The bare edge velocity v is determined solely by the gradient of the external potential that confines electrons within the system, which does not incorporate screening effects arising from the two-dimensional electron gas. This is the case even though it is expected, for realistic parameters, that the edges of a quantum Hall system are compressible and that screening by electrons within the edge is important, as represented by a Hartree potential that varies rapidly across the edge.[23] This Hartree contribution to the confining potential does not influence the velocity of modes with wavelength much longer than the width of a compressible edge, because when such modes are excited, the entire charge distribution within the compressible edge is displaced rigidly, carrying the Hartree potential with it.[24]

B. Correlation function

A central quantity in our calculation of transport properties is the one-particle correlation function in the absence of tunneling. Note that, without tunneling, the two edges may be in equilibrium with two separate reservoirs at different chemical potentials. We use the interaction representation, writing $\mathcal{O}(t) = e^{i\mathcal{H}_1 t/\hbar} \mathcal{O} e^{-i\mathcal{H}_1 t/\hbar}$. Thermal averages in the absence of tunneling are denoted by $\langle \cdots \rangle \equiv \text{Tr}(e^{-\beta\mathcal{H}_1} \cdots)/\text{Tr}(e^{-\beta\mathcal{H}_1})$. The one-electron correlation function we are concerned with is

$$G_m(x,t) \equiv \langle \psi_m^\dagger(x,t) \psi_m(0,0) \rangle. \quad (12)$$

We evaluate this in a standard way, using bosonization. As a first step, define the boson field operator

$$\phi_m(x) = -\sum_{q>0} \frac{1}{\sqrt{n_q}} (e^{-iqx} b_{q,m}^\dagger + e^{iqx} b_{q,m}) e^{-\epsilon q/2}, \quad (13)$$

where ϵ is an ultraviolet cut-off. This field obeys the commutation relation

$$[\phi_n(x), \partial_y \phi_m(y)] = -2\pi i \delta_{nm} \delta(x-y). \quad (14)$$

The fermion and boson field operators are related by

$$\psi_m(x) = \frac{F_m}{\sqrt{2\pi\epsilon}} e^{i2\pi\hat{N}_m x/L} e^{-i\phi_m(x)}, \quad (15)$$

where F_m is a Klein factor that satisfies the anticommutation relation $\{F_m^\dagger, F_n\} = 2\delta_{mn}$. The correlation function can be written as

$$G_m(x,t) = \frac{1}{2\pi\epsilon} e^{-i\mu_m x/(\hbar v)} \langle F_m^\dagger(t) F_m(0) \rangle \langle e^{i\phi_m(x,t)} e^{-i\phi_m(0,0)} \rangle. \tag{16}$$

The two expectation values are straightforward to evaluate. The one involving Klein factors yields

$$\langle F_m^\dagger(t) F_m(0) \rangle = e^{i\mu_m t/\hbar}. \tag{17}$$

To calculate the bosonic expectation value, it is useful to define the function $g_m(r,t)$ and its logarithm $S_m(r,t)$ via

$$g_m(x,t) \equiv \frac{1}{2\pi\epsilon} \langle e^{i\phi_m(x,t)} e^{-i\phi_m(0,0)} \rangle \equiv \frac{1}{(2\pi)} e^{S_m(x,t)}. \tag{18}$$

Since the bosonic Hamiltonian is quadratic, we can express $S_m(x,t)$ as

$$S_m(x,t) = -\ln \epsilon - \frac{1}{2}\langle [\phi_m(x,t) - \phi_m(0,0)]^2 \rangle$$
$$+ \frac{1}{2}[\phi_m(x,t), \phi_m(0,0)]. \tag{19}$$

The thermal average and the commutator appearing in this expression can be simplified via a mode expansion by expressing $\phi_m(x,t)$ in terms of boson creation and annihilation operators using Eq. (13). The boson correlation functions are independent of m, and so we drop the edge index. We find

$$S(x,t) = -\ln \epsilon - \int_0^\infty \frac{dq}{q} e^{-\epsilon q} (\coth[\beta\hbar\omega(q)/2]$$
$$\times \{1 - \cos[qx - \omega(q)t]\} - i\sin[qx - \omega(q)t]). \tag{20}$$

Combining these ingredients, we have

$$\langle \psi_m^\dagger(x,t)\psi_m(0,0)\rangle = \frac{1}{2\pi} e^{i\mu_m(t-x/v)/\hbar} e^{S(x,t)}. \tag{21}$$

By a similar calculation, we find

$$\langle \psi_m(x,t)\psi_m^\dagger(0,0)\rangle = \frac{1}{2\pi} e^{-i\mu_m(t-x/v)/\hbar} e^{S(x,t)}. \tag{22}$$

III. CONDUCTANCE AND NOISE POWER

In this section we express the differential conductance and noise power for the interferometer in terms of the correlation function evaluated in Sec. II B. As a first step, we require the operator $\hat{I}$ representing current from edge 1 to edge 2. It can be obtained from the time evolution of the total charge operator as

$$\hat{I} = -e\frac{d}{dt}\hat{N}_1 = -\frac{ie}{\hbar}[\mathcal{H},\hat{N}_1] = \frac{ie}{\hbar}[\mathcal{H},\hat{N}_2]$$
$$= \frac{e}{\hbar}\{it_a\psi_1^\dagger(0)\psi_2(0) + it_b\psi_1^\dagger(d_1)\psi_2(d_2) + \text{H.c.}\}. \tag{23}$$

A. Conductance

The expectation value for the current at time t is

$$I(t) = \langle \mathcal{U}(-\infty,t)\hat{I}(t)\mathcal{U}(t,-\infty)\rangle, \tag{24}$$

where $\mathcal{U}(t_2,t_1)$ is the operator for time evolution from time t_1 to t_2. In the interaction representation that we are using, it has the form $\mathcal{U}(t_2,t_1) = T_t \exp\left[-\frac{i}{\hbar}\int_{t_1}^{t_2}\mathcal{H}_{\text{tun}}(t)dt\right]$, where T_t denotes time ordering.

To lowest order in the tunneling we have

$$I(V) = -\frac{i}{\hbar}\int_{-\infty}^0 dt\langle[\hat{I}(0),\mathcal{H}_{\text{tun}}(t)]\rangle. \tag{25}$$

Using the correlation functions of Eqs. (21) and (22), the average current is

$$I(V) = \frac{-2e}{\hbar^2}\int_{-\infty}^{+\infty} dt((|t_a|^2 + |t_b|^2)e^{-i(\mu_1-\mu_2)t/\hbar}(i)\text{Im}[g(0,t)^2]$$
$$+ \{t_a t_b^* e^{i(\mu_1 d_1 - \mu_2 d_2)/\hbar v} e^{-ie(\mu_1-\mu_2)t/\hbar}(i)\text{Im}[g(d_1,t)g(d_2,t)]$$
$$+ \text{c.c.}\}). \tag{26}$$

The voltage applied to the interferometer is related to the chemical potentials of the edges by $V = (\mu_1 - \mu_2)/e$. The differential conductance $\sigma(V) \equiv dI(V)/dV$ has a contribution $\sigma_0(V)$, which is independent of the enclosed flux Φ, and another $\sigma_\Phi(V)$, which varies with Φ. Choosing μ_2 independent of V and introducing $G_0 = e^2/h$, the quantum unit of conductance, we find at leading order in tunneling

$$\sigma_0(V) = -4\pi G_0 \frac{|t_a|^2 + |t_b|^2}{\hbar^2}\int_{-\infty}^{+\infty} dt\, e^{-ieVt/\hbar} t\,\text{Im}[g(0,t)^2],$$

$$\sigma_\Phi(V) = -4\pi G_0\left\{\frac{t_a t_b^*}{\hbar^2}e^{i\mu_2(d_1-d_2)/\hbar v}\int_{-\infty}^{+\infty} dt\, e^{-ieVt/\hbar} t\right.$$
$$\left.\times\text{Im}[g(d_1,t+d_1/v)g(d_2,t+d_1/v)] + \text{c.c.}\right\}. \tag{27}$$

This is one of our central results. As in a noninteracting system, the differential conductance has zeroth and first harmonics in the flux ratio Φ/Φ_0, but with interactions their amplitudes acquire a bias dependence, which enters via the time dependence of the correlation function $g(x,t)$. We postpone a discussion both of this bias dependence and of the temperature dependence to Sec. V, after our analysis in Sec. IV of the correlation function. From the structure of the calculation, it is clear that at higher order in tunneling amplitudes, higher harmonics appear in the flux dependence of the differential conductance as a consequence of interactions.

B. Noise power

Now we turn to a calculation of the noise power $P(\omega, V)$ at frequency ω and voltage V, defined in terms of the current by

$$P(\omega, V) = \int_{-\infty}^{\infty} dt \, \cos(\omega t)[\langle \hat{I}(t)\hat{I}(0)\rangle - \langle \hat{I}(0)\rangle^2]. \quad (28)$$

Note that this includes contributions from both shot noise and Nyquist noise. At lowest order in the tunneling amplitude we need keep only the first term. We find

$$P(\omega, V) = \frac{2e^2}{\hbar^2} \int_{-\infty}^{+\infty} dt \, \cos(\omega t)((|t_a|^2 + |t_b|^2)e^{-ieVt/\hbar}$$
$$\times \mathrm{Re}[g(0,t)^2] + \{t_a t_b^* e^{i(\mu_1 d_1 - \mu_2 d_2)/\hbar v} e^{-ieVt/\hbar}$$
$$\times \mathrm{Re}[g(d_1,t)g(d_2,t)] + \text{c.c.}\}). \quad (29)$$

Hence, at leading order in tunneling, the flux dependence of the noise power has only zeroth and first harmonics. At higher order, we expect a second harmonic, as in the noninteracting system, and higher harmonics, as a consequence of interactions.

At leading order in tunneling, there is a version of the fluctuation-dissipation theorem that applies even at finite bias and that allows one to relate noise power to current.[25] It is derived as follows. First, introduce the operator $\mathcal{A}$ $= t_a \psi_1^\dagger(0)\psi_2(0) + t_b \psi_1^\dagger(d_1)\psi_2(d_2)$: we have $\mathcal{H}_{\mathrm{tun}} = \mathcal{A} + \mathcal{A}^\dagger$ and $\hat{I}$ $= (ie/\hbar)(\mathcal{A} - \mathcal{A}^\dagger)$. Then at leading order in tunneling

$$I(V) = -\frac{e}{\hbar^2} \int_{-\infty}^{\infty} dt \langle [\mathcal{A}^\dagger(t), \mathcal{A}(0)]\rangle. \quad (30)$$

In a similar fashion, the noise power at leading order is given by

$$P(\omega, V) = \frac{e^2}{\hbar^2} \int_{-\infty}^{\infty} dt \, \cos(\omega t)\langle \{\mathcal{A}^\dagger(t), \mathcal{A}(0)\}\rangle. \quad (31)$$

At this point it is useful to introduce a spectral decomposition of $\mathcal{A}$ in terms of the eigenstates of the Hamiltonian in absence of tunneling. Since the Hamiltonian in the absence of tunneling conserves the number of particles on each edge, one can use the basis $|\mathbf{n}\rangle = |E_{\mathbf{n}}, N_1, N_2\rangle$ for this spectral decomposition and define

$$A(\omega) = 2\pi Z^{-1} \sum_{\mathbf{n},\mathbf{m}} (e^{-\beta E_{\mathbf{n}}} + e^{-\beta E_{\mathbf{m}}})|\langle \mathbf{m}|\mathcal{A}|\mathbf{n}\rangle|^2$$
$$\times \delta(\hbar\omega + E_{\mathbf{n}} - E_{\mathbf{m}}), \quad (32)$$

where $Z = \sum_{\mathbf{n}} e^{-\beta E_{\mathbf{n}}}$. By rewriting the current and noise power in terms of the basis $|\mathbf{n}\rangle$, one can relate these two quantities to the spectral function:

$$I(V) = \frac{e}{\hbar} \tanh[\beta eV/2]A(eV/\hbar), \quad (33)$$

$$P(\omega, V) = \frac{e^2}{2\hbar}[A(eV/\hbar + \omega) + A(eV/\hbar - \omega)]. \quad (34)$$

We can therefore rewrite the power as

$$P(\omega, V) = \frac{e}{2} \sum_{\pm} \coth[\beta(eV \pm \hbar\omega)/2]I(V \pm \hbar\omega/e). \quad (35)$$

In particular, at zero temperature and zero frequency, we find $P(0,V)/eI(V) = 1$. As a result, at weak tunneling, noise power provides no extra information compared to conductance.

C. Voltage dependence

From Eq. (27) we see that the dependence on bias voltage V of conductance is given by Fourier transforms with respect to time t and with V as the transform variable, of combinations of the correlation function $g(x,t)$. A similar statement holds for noise power from Eq. (29), but with $V \pm \hbar\omega/e$ as the transform variable. For both conductance and noise power, there are two types of contribution: one independent of flux, which involves only $g(0,t)$, and one harmonic in Φ, which involves $g(d_1, t+d_1/v)$ and $g(d_2, t+d_1/v)$. For an interferometer with arm lengths much greater than the interaction range, there are distinct voltage scales associated with these two types of contribution. For definiteness, we discuss short-range interactions with a range b, as introduced above. Then a characteristic scale in the time dependence of $g(0,t)$ is b/v with a corresponding voltage scale $\hbar v/eb$. This is the relevant scale for the flux-independent contributions to conductance and noise power: it marks a crossover between separate regimes of free electron behavior at low and high bias. At low bias, the relevant edge velocity is v, while at high bias the velocity acquires a finite renormalization from interactions and is $v - u(0)$. In the following, we restrict ourselves to the low-bias regime, so that flux-independent quantities have negligible variation with V. In this regime, we focus on the voltage dependence of Aharonov-Bohm oscillations in conductance and noise power, which is determined by the time dependence of $g(d_1, t+d_1/v)$ and $g(d_2, t+d_1/v)$. As we show below, with $x \gg b$, there is a much larger characteristic time scale for $g(x,t)$ than for $g(0,t)$, and so the voltage scale relevant to the Aharonov-Bohm oscillations is much smaller than $\hbar v/eb$.

IV. ASYMPTOTICS OF THE CORRELATION FUNCTION

In order to obtain the voltage dependence of Aharonov-Bohm oscillations in conductance and noise power, we need to evaluate, for large fixed $|x|$ as a function of t, the correlation function $g(x,t)$ by computing the integral on q in Eq. (20). We will find that interactions generate x-dependent length and time scales ℓ and t_φ, which characterize the width and duration of an electron wave packet passing the point x after injection at the origin. In addition, at finite temperature a dephasing length ℓ_φ arises. It is worthwhile to compare dephasing in the interferometer with the situation in a conventional mesoscopic conductor treated using linear response theory. In the interferometer, dephasing may arise either from finite bias voltage or from thermal excitations: it is therefore characterized by two distinct scales t_φ and ℓ_φ. By contrast, within linear response dephasing is due only to thermal excitations, and length and time scales for dephasing are simply related. Finally, it is convenient to parametrize tem-

perature in terms of a thermal length $L_T \equiv \hbar v \beta$ defined for the noninteracting system.

At large $|x|$ the dominant contribution to Eq. (20) is from small q, and so we are concerned with the form of $\omega(q)$ at small q. We consider separately the cases of short-range interactions, and of Coulomb interactions. For the first, we have

$$\omega(q) = vq - (v/b)(bq)^n \cdots ,$$

with $n = 3$. We obtain [see Eq. (45)] $\ell \equiv b(x/b)^{1/n}$, with

$$t_\varphi \equiv \ell/v \qquad (36)$$

and

$$\ell_\varphi = L_T (L_T/b)^{n-1}. \qquad (37)$$

To understand the physical origin of the dependence of t_φ on x, consider an electron wave packet of width ℓ. It consists of modes with wave vectors in a range from 0 to $\mathcal{O}(1/\ell)$. The phase difference accumulated due to dispersion, between modes at opposite ends of this range, during propagation over the distance x, is $(v/b)(b/\ell)^n(x/v)$, and the value of ℓ may be extracted from the consistency requirement that this phase difference is $\mathcal{O}(1)$.

In the case of Coulomb interactions, we have

$$\omega(q) = q[v + u \ln(1/aq)].$$

We find [see Eq. (48)] $\ell = x/\ln(x/a)$,

$$t_\varphi = \ell/[u \ln(\ell/a)], \qquad (38)$$

and

$$\ell_\varphi = (uL_T/v) \cdot \ln^2(L_T/a). \qquad (39)$$

In addition to dephasing of this kind, due to interactions, there may be dephasing of collective bosonic modes that arises from the curvature of the single-particle dispersion relation for edge electrons, which was omitted from Eq. (2). Such curvature generates cubic and higher-order terms in the bosonic Hamiltonian and hence scattering between collective modes.[26] We estimate the dephasing length $\ell_\varphi^{\mathrm{curv}}$ arising from this mechanism as follows. First, we parametrize the curvature in the electron dispersion in terms of a length scale $|D|$ by writing in place of Eq. (2):

$$\mathcal{H}_0 = \hbar v \sum_{qm} \left(q + \frac{l_B^2 q^2}{D} + \cdots \right) c_{qm}^\dagger c_{qm},$$

where l_B is the magnetic length. Following the discussion of a compressible quantum Hall edge given in Ref. 23, one expects $|D|$ to be of the order of the depletion length. A consequence of this curvature is of course that electrons travel at different speeds according to their energy. Thermally excited electrons occupy a wave-vector range $\Delta q \sim L_T^{-1}$ and hence have a velocity range $\Delta v \sim v l_B^2/(|D|L_T)$. The dephasing length is the distance that electrons with wave vectors differing by Δq must propagate to acquire a phase difference $\mathcal{O}(\pi)$, and so

$$\ell_\varphi^{\mathrm{curv}} = \frac{v}{\Delta q \Delta v} = |D| \left(\frac{L_T}{l_B} \right)^2. \qquad (40)$$

Equivalent results have been derived previously for a nonchiral system by treating cubic interactions between bosonic modes perturbatively,[27] and a discussion including the effects of disorder is given in Ref. 28.

Let us summarize the outcome of our discussion of dephasing lengths important for the correlation function. Shortrange interactions [$n = 3$ in Eq. (37)] give

$$\ell_\varphi \propto T^{-3}, \qquad (41)$$

while, from Eq. (40), curvature in the fermion disperison relation leads to

$$\ell_\varphi^{\mathrm{curv}} \propto T^{-2}. \qquad (42)$$

With short-range interactions, the effects of curvature are therefore dominant in the low-temperature limit, but $\ell_\varphi < \ell_\varphi^{\mathrm{curv}}$ and interaction effects dominate above the temperature at which $L_T = |D|(b/l_B)^2$. By contrast, for Coulomb interactions, from Eq. (39),

$$\ell_\varphi \propto T^{-1} \ln^2(1/T), \qquad (43)$$

and so dephasing from interactions dominates over curvature effects at low temperatures. We discuss numerical estimates for dephasing lengths in Sec. VI.

Moving to details of the evaluation of the asymptotic form at large x of the correlation function for an interacting system with linear electron dispersion, there are two separate regimes, according to whether $|x - vt|$ is small or large compared to ℓ.

A. Far from the peak: $|x - vt|$ large

Then it is sufficient to approximate the dispersion relation as $\omega(q) = vq$, and one obtains the correlation function for noninteracting particles with speed v, which is

$$g(x,t) = \frac{i\pi k_B T/\hbar v}{2\pi \sinh([x - vt]\pi k_B T/\hbar v)}. \qquad (44)$$

B. Near the peak: $|x - vt|$ small

In this regime it is necessary to take account of the leading correction at small q to a strictly linear dispersion relation, which we do separately for short-range and for Coulomb interactions.

1. Short-range interactions

We write $t = \Delta t + x/v$, so that at leading order

$$qx - \omega(q)t = \frac{x}{b}(bq)^n - qv \, \Delta t \cdots ,$$

and rescale variables, using ℓ and t_φ to define the dimensionless combinations:

$$\ell q \equiv Q, \quad \Delta t/t_\varphi \equiv \tau,$$

$$\epsilon/\ell \equiv \epsilon', \quad \beta\hbar/t_\varphi \equiv \beta'.$$

Then

$$qx - \omega(q)t = (\ell q)^n - \ell q \Delta t/t_\varphi \cdots . \tag{45}$$

We obtain from Eq. (20)

$$S(x,t) = -\ln(\ell) - \ln(\epsilon') + \int_0^\infty \frac{dQ}{Q} e^{-\epsilon' Q}\{\coth(\beta' Q/2)$$

$$\times [\cos(Q^n - \tau Q) - 1] + i\sin(Q^n - \tau Q)]\}.$$

We can remove the ϵ' dependence by using the result that, as $\epsilon' \to 0$,

$$-\ln(\epsilon') + \int_0^\infty \frac{dQ}{Q} e^{-\epsilon' Q} \coth(\beta Q/2)[\cos(Q) - 1]$$

$$= \ln\left[\frac{\pi/\beta}{\sinh(\pi/\beta)}\right] \tag{46}$$

to write

$$S(x,t) = -\ln(\ell) + \ln\left[\frac{\pi/\beta'}{\sinh(\pi/\beta')}\right] + \int_0^\infty \frac{dQ}{Q}\{\coth(\beta' Q/2)$$

$$\times [\cos(Q^n - \tau Q) - \cos(Q)] + i\sin(Q^n - \tau Q)]\}. \tag{47}$$

From the asymptotic behavior of Eq. (47) at large $|\tau|$, one can recover the form for the correlation function at large $|x - vt|$ given in Eq. (44).

The analysis leading to Eq. (47) makes clear the scales that are important for $g(x,t)$. Considered as a function of t at large, fixed x, $g(x,t)$ has a peak near $t = x/v$. The peak has a width in t of order ℓ/v and near the peak $|g(x,t)| \sim \ell^{-1}$. The interaction energy scale that enters the temperature or voltage dependence of the interferometer fringe visibility is $\hbar/t_\varphi$. Correspondingly, at a given inverse temperature β, fringes are visible only for $\ell \lesssim \beta\hbar v$, from which we see that the dephasing length is as given in Eq. (37). To find the detailed asymptotic form of the correlation function, it is necessary to evaluate Eq. (47) numerically.

2. Unscreened Coulomb interactions

Starting from $\omega(q) = q[v_0 + u\ln(1/aq)]$, we would again like a simplified asymptotic form for the correlation function at large $|x|$ and $|t|$. Without screening, the phase velocity is $v + u\ln(1/aq)$ and hence divergent at small q. Focusing on behavior near the peak of the correlation function, we write $t = \Delta t + x/[v + u\ln(x/a)]$ so that

$$qx - \omega(q)t = \frac{qux\ln(qx)}{v + u\ln(x/a)} - q[v + u\ln(1/qa)]\Delta t.$$

We assume for simplicity that $u\ln(x/a) \gg v$ (though this is not essential) and introduce the characteristic length $\ell = x/\ln(x/a)$ and time $t_\varphi = \ell/[u\ln(\ell/a)]$. Then

$$qx - \omega(q)t = \ell q \ln(\ell q) - \ell q \Delta t/t_\varphi \cdots . \tag{48}$$

Defining dimensionless variables as before, the asymptotic form of the correlation function is obtained from
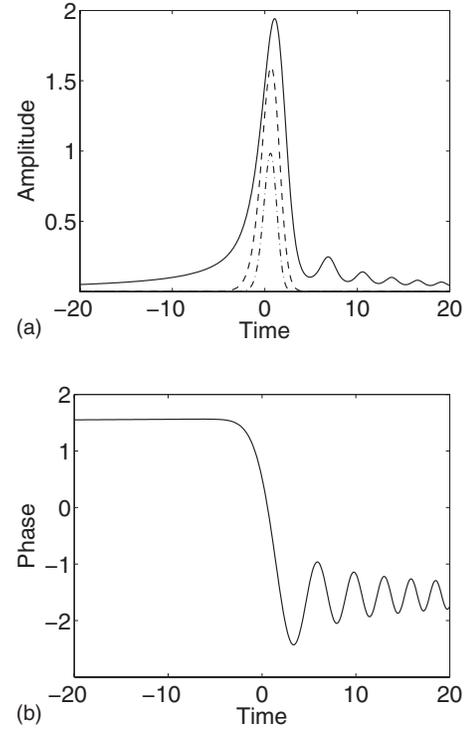

(a)

(b)

FIG. 4. Asymptotic behavior of the correlation function for short-range interactions. Upper panel: the function $\exp[U(\beta', \tau)]$, proportional to its modulus, as a function of τ, for $\beta' = \infty$ (solid line), $\beta' = 2$ (dashed line), and $\beta' = 1$ (dash-dotted line). Lower panel: its phase $W(\tau)$.

$$S(x,t) = -\ln(\ell) + \ln\left[\frac{\pi/\beta'}{\sinh(\pi/\beta')}\right]$$

$$+ \int_0^\infty \frac{dQ}{Q}(\coth(\beta' Q/2)\{\cos[Q\ln(Q) - Q\tau]$$

$$- \cos(Q)\} + i\sin[Q\ln(Q) - Q\tau]). \tag{49}$$

In this way we see for Coulomb interactions, taking the energy scale for visibility of interference fringes as $\hbar/t_\varphi$, that the dephasing length is as in Eq. (39).

C. Numerical evaluation of the asymptotic form for the correlation function

For both short-range interactions and Coulomb interactions it is convenient to write

$$S(x,t) = -\ln(\ell) + U(\beta', \tau) + iW(\tau),$$

where $U(\beta', \tau)$ and $W(\tau)$ are each real and can be read off from Eqs. (47) and (49). The modulus of the correlation function is proportional to $\exp[U(\beta', \tau)]$, and its phase is $W(\tau)$. These functions are shown in Fig. 4 for short-range interactions with $n = 3$ and in Fig. 5 for Coulomb interactions.

V. VISIBILITY OF INTERFERENCE FRINGES

Coherence in the interferometer can be characterized by the interference fringe visibility, defined as
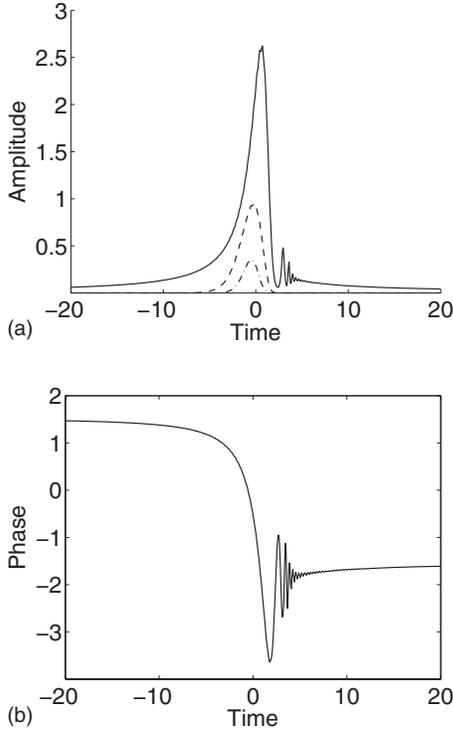
FIG. 5. Asymptotic behavior of the correlation function for Coulomb interactions. Upper panel: the function $\exp[U(\beta', \tau)]$, proportional to its modulus, as a function of τ, for $\beta' = \infty$ (solid line), $\beta' = 2$ (dashed line), and $\beta' = 1$ (dash-dotted line). Lower panel: its phase $W(\tau)$.

$$\mathcal{V} = \frac{\max_\Phi \sigma(V) - \min_\Phi \sigma(V)}{\max_\Phi \sigma(V) + \min_\Phi \sigma(V)}. \qquad (50)$$

To provide a context for discussion of interaction effects, it is useful to recall the result of single-particle theory for the source-drain transmission probability of electrons with wave vector k. In terms of transmission and reflection amplitudes $\tau_{a,b}$ and $r_{a,b}$ at the point contacts a and b, this is[1]

$$|\tau_a r_b e^{ikd_2} + r_a \tau_b e^{ikd_1}|^2. \qquad (51)$$

It is characterized by the energy scale $E_c \equiv \hbar v / |d_1 - d_2|$, which is divergent for an interferometer with equal arm lengths. In a noninteracting system, the amplitude of Aharonov-Bohm oscillations in the differential conductance of the interferometer is independent of bias V and has a phase eV/E_c. Oscillations are suppressed at high temperature by thermal smearing with a characteristic temperature scale set by E_c, and the visibility is

$$\mathcal{V} = \frac{2|\tau_a \tau_b r_a r_b|}{|\tau_a|^2 |r_b|^2 + |\tau_b|^2 |r_a|^2} \frac{\pi k_B T / E_c}{\sinh(\pi k_B T / E_c)}. \qquad (52)$$

Turning to interaction effects, we find in general at leading order in tunneling that

$$\mathcal{V} = \frac{2|t_a t_b|}{|t_a|^2 + |t_b|^2} \mathcal{V}_{\rm rel}(V', \beta'), \qquad (53)$$

where V' and β' are scaled voltage and inverse temperature, respectively. In the limit of vanishing temperature and voltage, nonlinearity in the dispersion relation for bosonic excitations is not probed and so $\mathcal{V}_{\rm rel}(0, \infty) = 1$; away from this limit, we compute its form numerically. Because the asymptotic form of the correlation function depends on interactions only via the functional form of $u(q)$ at small q and the values of ℓ and τ_φ, numerical calculations yield universal results as a function of scaled voltage and temperature. These results apply provided the interferometer arms are much longer than the interaction length b. It is also possible to evaluate our expressions numerically for shorter arm lengths, without using the discussion of Sec. IV: our exploratory studies yielded results similar to the ones for the asymptotic regime of large arm length, presented below.

We discuss separately the two cases of interferometers with equal or unequal arm lengths. In each case, as noted at the end of Sec. III, for an interferometer with arm lengths large compared to the interaction range, $\sigma_0(V)$ is almost constant over the bias range of interest, so that the visibility of interference fringes in conductance is determined directly by $\sigma_\Phi(V)$.

A. Interferometer with arms of equal length

1. Zero temperature

From Eq. (27), the oscillatory part of the conductance can be written as

$$\sigma_\Phi(V) = A(\sigma_1(V) + i\sigma_2(V) + \text{c.c.}),$$

where $A = -2G_0 \ell t_a t_b^* / (v\hbar)^2$ and

$$\sigma_1(V') + i\sigma_2(V') = \int_{-\infty}^{\infty} d\tau \exp(-iV'\tau)\tau$$
$$\times \exp[2U(\beta', \tau)]\sin[2W(\tau)],$$

with the scaled voltage $V' = eVt_\varphi/\hbar$. The amplitude of oscillations has modulus $\sigma(V) = \sqrt{\sigma_1^2(V) + \sigma_2^2(V)}$.

The resulting visibility $\mathcal{V}_{\rm rel}(V', \beta')$ and the separate contributions derived from $\sigma_1(V)$ are $\sigma_2(V)$, are shown in Fig. 6. A striking feature is that for intermediate V, the visibility at low temperature exceeds unity: this means that in this bias range, for some values of Φ, the differential conductance is negative.

2. Nonzero temperature

Temperature enters these calculations via the β' dependence of $U(\beta', \tau)$. The effect of this on the modulus of the Green function is shown in Figs. 4 and 5. The resulting visibility is shown in Fig. 7.

B. Interferometer with arms of different lengths

For an interferometer with different arm lengths, the oscillatory part of the conductance is proportional to
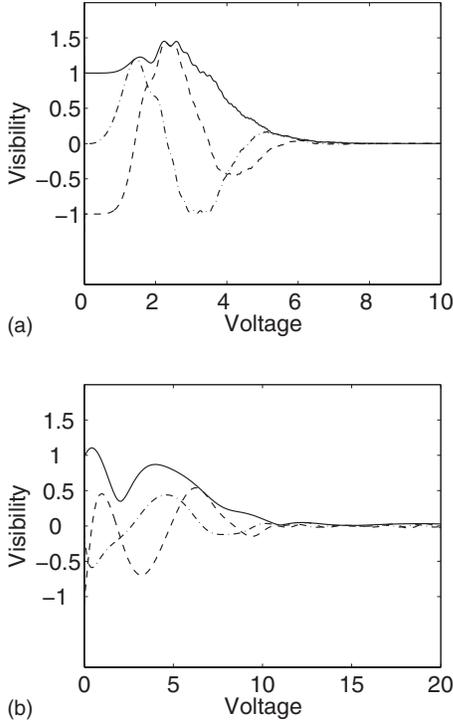
FIG. 6. The voltage dependence of visibility for equal length arms at zero temperature. Upper panel: with short-range interactions. Lower panel: with Coulomb interactions. Solid lines: $\mathcal{V}_{\text{rel}}(V',\beta')$. Dashed lines and dot-dashed lines: contributions from $\sigma_1(V)$ and $\sigma_2(V)$, respectively.

$$\int_{-\infty}^{\infty} dt \, \exp(-ieVt/\hbar)t \, \text{Im}[g(d_1, t+d_1/v)g(d_2, t+d_1/v)].$$

Since $g(x,t)$ away from its peaks is asymptotically pure imaginary, the only contributions to $\text{Im}[g(d_1, t+d_1/v)g(d_2, t+d_1/v)]$ are from the regions of t close to the peak of one or other correlation function. We introduce ℓ_1 and ℓ_2, obtained from ℓ by setting $x=d_1$ and $x=d_2$, respectively. Similarly, we define $t_{\varphi 1}$ and $t_{\varphi 2}$. The peak in $g(d_1, t+d_1/v)$ occurs near $t=0$. Close to this peak we can write $t=\tau t_{\varphi 1}$ and approximate

$$g(d_1, t+d_1/v) \approx \frac{1}{2\pi\ell_1} \exp[U(\beta',\tau) + iW(\tau)],$$

$$g(d_2, t+d_1/v) \approx \frac{i\pi k_B T/\hbar v}{2\pi \sinh([d_2-d_1]\pi k_B T/\hbar v)}.$$

The peak in the other correlation function, $g(d_2, t+d_1/v)$, is near $t=(d_2-d_1)/v$. Close to this peak, we can write $t=(d_2-d_1)/v + \tau t_{\varphi 2}$ and approximate

$$g(d_1, t+d_1/v) \approx -\frac{i\pi k_B T/\hbar v}{2\pi \sinh([d_2-d_1]\pi k_B T/\hbar v)},$$
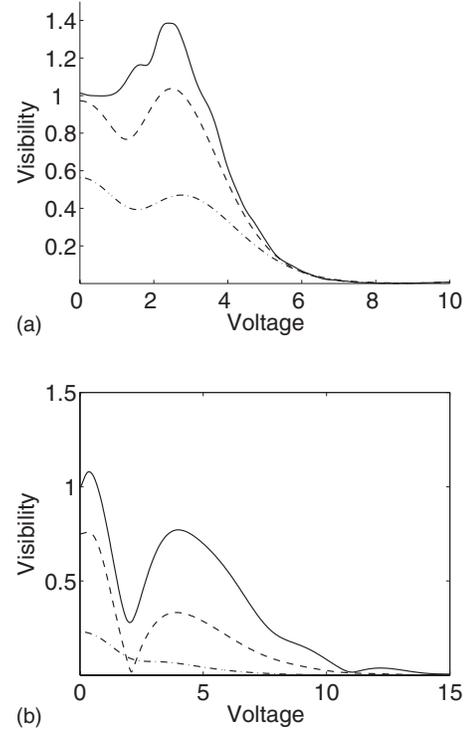

FIG. 7. The dependence of $\mathcal{V}_{\text{rel}}(V',\beta')$ on V' for equal arm lengths at $\beta'=20$ (solid line), $\beta'=5$ (dashed line), and $\beta'=2$ (dot-dashed line). Upper panel: short-range interactions. Lower panel: Coulomb interactions.

$$g(d_2, t+d_1/v) \approx \frac{1}{2\pi\ell_2} \exp[U(\beta',\tau) + iW(\tau)].$$

The combination $t \, \text{Im}[g(d_1, t+d_1/v)g(d_2, t+d_1/v)]$ is larger near the second peak than the first by a factor $(d_2-d_1)/\ell_1$, because t is larger in this case. When evaluating this contribution, we need to introduce a scaled voltage $V' = (eVt_{\varphi 2}/\hbar)$ and a scaled length difference $\lambda=(d_2-d_1)/\ell_2$. Then the leading contribution to the integrand in Eq. (54) for d_1 and d_2 large is

$$\exp(-ieVt/\hbar)t \, \text{Im}[g(d_1, t+d_1/v)g(d_2, t+d_1/v)]$$

$$= \exp(-i\lambda V')\exp(-iV'\tau)\frac{d_1-d_2}{v}$$

$$\times \frac{\pi k_B T/\hbar v}{(2\pi)^2 \sinh([d_2-d_1]\pi k_B T/\hbar v)}\frac{1}{\ell_2}$$

$$\times \exp[U(\beta',\tau)]\cos[V(\tau)]. \tag{54}$$

The factors on the right-hand side of Eq. (54) from the two correlation functions lead to suppression of conductance oscillations by two different mechanisms: thermal smearing, governed by the parameter $k_B T(d_2-d_1)/\hbar v$, and interaction effects, governed by $k_B T t_{\varphi 2}/\hbar$. Unless d_2-d_1 is parametrically smaller than d_2, thermal smearing dominates and the behavior at nonzero temperature is obtained simply by multiplying the zero-temperature results by the factor $[\pi k_B T/\hbar v]/[(2\pi)^2 \sinh([d_2-d_1]\pi k_B T/\hbar v)]$. Results for con-
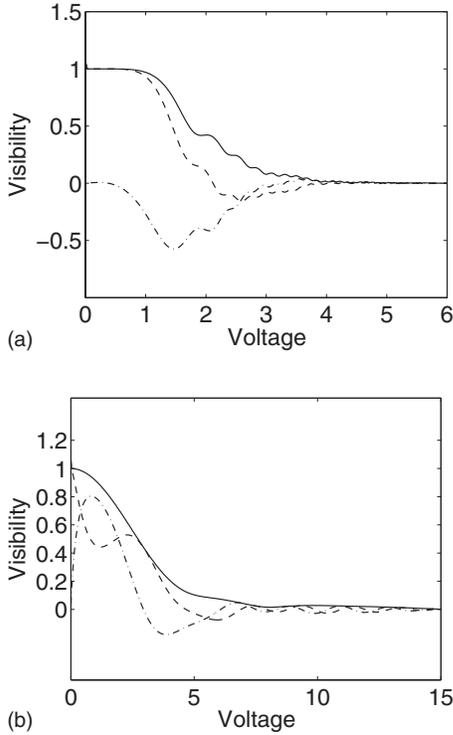
FIG. 8. The voltage dependence of visibility for an interferometer having arms of different lengths at zero temperature. Upper panel: short-range interactions. Lower panel: Coulomb interactions. Solid lines: $\mathcal{V}_{\text{rel}}(V', \beta')$. Dashed lines and dot-dashed lines: contributions from $\sigma_1(V)$ and $\sigma_2(V)$, respectively.

ductance as a function of voltage at zero temperature are shown in Fig. 8.

VI. DISCUSSION

In summary, we have shown using a microscopic treatment of electron-electron interactions how, at finite bias or temperature, these interactions influence Aharonov-Bohm oscillations in conductance and noise power for a Mach-Zehnder interferometer. The visibility of oscillations in both quantities at weak tunneling is determined by the correlation function for electrons in a quantum Hall edge state, and we have analyzed the form of this correlation function for systems with short-range interactions or with unscreened Coulomb interactions. Measurement of the visibility of oscillations as a function of bias in an interferometer with arms of equal length should provide a means to determine this correlation function.

Visibility is suppressed both at high bias and at high temperature. The voltage scale for the bias dependence of visibility is set by the time scale t_φ, given in Eqs. (36) and (38). Suppression of visibility with temperature arises both from dephasing by interactions, also on a scale set by t_φ, and—in an interferometer with arms of different lengths—from thermal smearing, a single-particle effect. A similar combination of dephasing and thermal smearing contributions is well known in the temperature dependence of mesoscopic conductance fluctuations.[29] For the interferometer, thermal

smearing dominates over dephasing unless the difference in arm lengths is small.

A discussion of numerical values for dephasing lengths is made difficult by uncertainty in the value of the edge velocity v. An experimental study[30] of edge magnetoplasmons yields a velocity of about 2.5×10^4 m s^{-1} in GaAs with a field of 5 T at filling factor $\nu = 1$. Alternatively, an upper limit is $v \sim \omega_c l_B$, where ω_c is the cyclotron frequency; taking the effective mass of electrons in GaAs and a field of 4 T, this yields $v \sim 1.4 \times 10^5$ m s^{-1}. The resulting value of the thermal length at a temperature of 100 mK is $L_T = 10$ μm. At this temperature the dephasing length due either to short-range interactions or to curvature in the electron disperison relation far exceeds experimental sample dimensions. To see this, consider for definiteness an edge state confined by a metallic gate and suppose that Coulomb interactions are screened by this gate so that the interaction range is set by the depletion length: $b \sim D \sim 200$ nm. Then, from Eq. (37) with $n = 3$, $\ell_\varphi \sim 25$ mm, while $\ell_\varphi^{\text{curv}} \sim 1$ mm. By contrast, the dephasing length due to unscreened Coulomb interactions, being only logarithmically larger than L_T, is comparable to the sample dimensions and may be smaller if the true value of v is smaller. Consistency with experiment therefore requires use of unscreened Coulomb interactions in the theory we have developed. We note that sample edges in the experiments of Refs. 1–3 are defined mainly by etching, so that interactions within the edge states are likely to be poorly screened.

Earlier work has treated dephasing more phenomenologically, via a fictitious dephasing voltage probe[16] or a fluctuating external potential.[13–15,17] Our results from a microscopic approach complement this earlier work in several important ways. First, we connect the voltage and temperature scales for suppression of Aharonov-Bohm oscillations with parameters characterizing the system at a microscopic level: the edge velocity and the interaction range. Second, we demonstrate that the temperature dependence of the dephasing length depends very much on the nature of electron-electron interactions within the system: with realistic parameter choices, interactions that are short range because of external screening generate negligible dephasing, while unscreened Coulomb interactions are much more effective in reducing coherence. Third, we show that the functional form of the dependence of visibility with temperature or voltage varies significantly according to the model chosen for interactions and so provides a useful window through which details of scattering processes can be viewed.

Turning to a comparison of our results with the experimental observations of Refs. 1–3 while our calculations capture the central phenomenon of suppression of visibility with either increasing temperature or increasing bias,[1] there are also features that we cannot account for and others that we cannot make contact with, because our calculations are at leading order in tunneling amplitudes. In more detail, some successes and limitations are as follows. In Ref. 1, suppression of the visibility of oscillations in the differential conductance is observed, with the same energy scale entering both temperature and voltage dependence. Our calculations reproduce this provided the interferometer is taken to have equal-length arms. In the same paper, it is suggested that noise power retains coherent features at a bias large enough to

suppress visibility in differential conductance. The observations concerned were made with $|\tau_b|^2=0.5$, which places them far outside the regime in which our results can be applied; nevertheless, we note that such behavior is in contrast to our results, in the sense that a common scale enters the visibility of oscillations in conductance and noise. The idea that there is a common scale for both quantities is in qualitative agreement with a more recent set of data.[3] In Ref. [2], very striking lobes were reported in visibility as a function of bias at low temperature. It is noteworthy that the dependence we find of visibility on bias is not in all cases simply a monotonic decrease and, for Coulomb interactions and equal arm lengths (Fig. [7]), shows pronounced peaks and minima. Within our calculations, these oscillations appear because visibility is given by a Fourier transform of the correlation function representing propagation of an injected electron along one arm of the interferometer and because the injected electron is represented by a pulse with a rather sharp trailing edge. It is tempting to relate these calculated oscillations to the observed lobes. However, a further key observation[2] is that a change in length for one of the interferometer arms leads to a reduction in the amplitude of these lobes in visibility, without a change in their period, while our calculations give no such lobes in an interferometer with arms of substantially different length (see Fig. [8]). For future work, there would be great interest in studying more realistic models of interactions, perhaps taking better account of the geometry of the sample, to see whether visibility lobes are a robust consequence.

ACKNOWLEDGMENTS

[1] Y. Ji, Y. C. Chung, D. Sprinzak, M. Heiblum, D. Mahalu, and H. Shtrikman, Nature (London) **422**, 415 (2003).

[2] I. Neder, M. Heiblum, Y. Levinson, D. Mahalu, and V. Umansky, Phys. Rev. Lett. **96**, 016804 (2006).

[3] I. Neder, M. Heiblum, D. Mahalu, and V. Umansky, Phys. Rev. Lett. **98**, 036803 (2007).

[4] L. V. Litvin, H.-P. Tranitz, W. Wegscheider, and C. Strunk, Phys. Rev. B **75**, 033315 (2007).

[5] F. E. Camino, W. Zhou, and V. J. Goldman, Phys. Rev. B **72**, 075342 (2005); Phys. Rev. Lett. **95**, 246802 (2005).

[6] T. Jonckheere, P. Devillard, A. Crepieux, and T. Martin, Phys. Rev. B **72**, 201305(R) (2005).

[7] K. T. Law, D. E. Feldman, and Y. Gefen, Phys. Rev. B **74**, 045319 (2006).

[8] E. A. Kim, M. J. Lawler, S. Vishveshwara, and E. Fradkin, Phys. Rev. B **74**, 155324 (2006).

[9] D. E. Feldman and A. Kitaev, Phys. Rev. Lett. **97**, 186803 (2006).

[10] V. V. Ponomarenko and D. V. Averin, arXiv:cond-mat/0612607 (unpublished).

[11] D. E. Feldman, Y. Gefen, A. Kitaev, K. T. Law, and A. Stern, arXiv:cond-mat/0612608 (unpublished).

[12] C. de C. Chamon, D. E. Freed, S. A. Kivelson, S. L. Sondhi, and X. G. Wen, Phys. Rev. B **55**, 2331 (1997).

[13] G. Seelig and M. Büttiker, Phys. Rev. B **64**, 245313 (2001).

[14] F. Marquardt and C. Bruder, Phys. Rev. Lett. **92**, 056805 (2004); Phys. Rev. B **70**, 125305 (2004).

[15] H. Förster, S. Pilgram, and M. Büttiker, Phys. Rev. B **72**, 075301 (2005).

[16] V. S.-W. Chung, P. Samuelsson, and M. B. Büttiker, Phys. Rev. B **72**, 125320 (2005).

[17] F. Marquardt, Europhys. Lett. **72**, 788 (2005); F. Marquardt, Phys. Rev. B **74**, 125319 (2006).

[18] I. Neder and F. Marquardt, New J. Phys. **9**, 112 (2007).

[19] X. G. Wen, Phys. Rev. Lett. **64**, 2206 (1990); Phys. Rev. B **43**, 11025 (1991).

[20] J. W. Tomlinson, J.-S. Caux, and J. T. Chalker, Phys. Rev. Lett. **94**, 086804 (2005); Phys. Rev. B **72**, 235307 (2005).

[21] E. V. Sukhorukov and V. V. Cheianov, arXiv:cond-mat/0609288 (unpublished).

[22] J. von Delft and H. Schoeller, Ann. Phys. (Leipzig) **7**, 225 (1998).

[23] D. B. Chklovskii, B. I. Shklovskii, and L. I. Glazman, Phys. Rev. B **46**, 4026 (1992).

[24] J. H. Han and D. J. Thouless, Phys. Rev. B **55**, R1926 (1997).

[25] D. Rogovin and D. J. Scalapino, Ann. Phys. (N.Y.) **86**, 1 (1974); E. V. Sukhorukov and D. Loss, in *Rencontres de Moriond XXXVI*, edited by G. Montambaux and T. Martin (EDP Sciences, Paris, 2001).

[26] F. D. M. Haldane, J. Phys. C **14**, 2585 (1981).

[27] K. V. Samokhin, J. Phys.: Condens. Matter **10**, L533 (1998).

[28] I. V. Gornyi, A. D. Mirlin, and D. G. Polyakov, Phys. Rev. B **75**, 085421 (2007).

[29] B. L. Altshuler and D. E. Khmel'nitskii, JETP Lett. **42**, 359 (1985); P. A. Lee, A. D. Stone, and H. Fukuyama, Phys. Rev. B **35**, 1039 (1987).

[30] R. C. Ashoori, H. L. Stormer, L. N. Pfeiffer, K. W. Baldwin, and K. West, Phys. Rev. B **45**, R3894 (1992).